

A TWO DIMENSIONAL SHOCK CAPTURING, HYDRODYNAMIC MODEL OF THE VENUS IONOSPHERE

 A. F. Nagy, A Körösmezey¹, J. Kim and T. I. Gombosi

Space Physics Research Laboratory, The University of Michigan

Abstract A two-dimensional, time-dependent, shock capturing single-species (O^+) hydrodynamic model of the Venus ionosphere, which solves the coupled continuity, momentum and energy equations for the altitude range of 150 - 500 km and the solar zenith angle range of 0° - 180° has been developed and is presented in this paper. It was again demonstrated that the introduction of topside heat inflows leads to calculated dayside electron and ion temperatures, which are consistent with the measured values. In order to reproduce the measured electron temperatures, which are roughly constant over all SZA's, the heat inflows had to be reduced significantly over the nightside compared to the dayside values. The calculated transterminator ion flows are supersonic and relatively close to the observed average values. The model predicts a deceleration shock at a SZA of about 135° , consistent with the ion temperature and velocity observations.

Introduction

Our understanding of the controlling physical and chemical processes in the ionosphere of Venus has advanced significantly since the launch of the Pioneer Venus Orbiter (PVO) [Colin, 1980]. The discovery of the transonic flow directed from the dayside toward the nightside of the Venus ionosphere was one of the many surprising facts that PVO established [Knudsen et al., 1980]. The typical high altitude transterminator ion velocities were found to be of the order of 2-3 km/s and are supersonic across the terminator at high altitudes. The ion flow is driven predominantly by the large pressure gradient, which is present across the terminator [Knudsen et al., 1981]. The rapid rise in ion temperatures and drop/randomization in ion velocities beyond a zenith angle of about 150° , led Knudsen et al., [1980] to suggest a shock deceleration of the supersonic flow deep on the nightside.

A number of models have been developed to study and establish the mechanisms responsible for these supersonic ion flows, but all of these previous transport models had some limitations (e.g. use of assumed velocity components, limited spatial coverage, lack of shock "capturing" ability). The need for a full-scale, two-dimensional, shock capturing model has been obvious for many years. However two dimensional models capable of such calculations are very complex and computer intensive and have only begun to be employed in the field of space plasma physics relatively recently [e.g. Gombosi et al., 1985]. A two-dimensional, time-dependent, shock capturing single-species (O^+) hydrodynamic model of the Venus ionosphere, which solves the coupled continuity, momentum and energy equations for the altitude range of 150 - 500 km and the solar zenith angle range of 0° - 180° has been developed and is presented in this paper. This two-dimensional model will help us to evaluate the importance of supersonic day-to-night flows and, for the first time address, in a quantitative way, the probability of shock formation in the nightside ionosphere of Venus.

Model Description

Governing Equations

The time-dependent two-dimensional continuity, momentum and energy equations for O^+ ions and electrons are solved self-consistently. Quasi-neutrality is assumed, i.e. $n_i = n_e$, where n denotes number density. Furthermore, the ion and electrons are assumed to have the same velocity, i.e. $u_{ion} = u_{electron}$, in other words the current is assumed to be zero. Knudsen et al. [1981] have shown that the transterminator flow is not strongly influenced by the magnetic field; therefore, the use of a hydrodynamic approach, assumed in this model, is sufficient to elucidate the important aspects of the high speed ion flow. The bulk motion of the neutral atmosphere is neglected. This is a reasonable assumption, because, in general, the ion velocities are significantly larger than the neutral ones. The assumption of only a single ion species, O^+ , was necessary in order to make the numerical solution "feasible". However this is a reasonably good assumption, because above about 190 km, O^+ is the dominant ion species and the main aim of these calculations is to establish the ion flows and their effect, which become significant only above about 200 km. The chemical reactions included in the model are listed in Table 1. In calculating the chemical source for O^+ from reaction (R1), the $[CO_2^+]$ density was approximated from the photochemical equilibrium relationship:

$$[CO_2^+] \cong \frac{P(CO_2^+)}{(k_1 + k_2)[O] + k_3[n_e]} \quad (1)$$

where $P(CO_2^+)$ is the photoionization rate of CO_2^+ . The continuity equation is:

$$\frac{\partial \rho}{\partial t} + \frac{1}{A_r} \frac{\partial}{\partial r} (A_r \rho u_r) + \frac{1}{r A_\theta} \frac{\partial}{\partial \theta} (A_\theta \rho u_\theta) = S_c - S_1 \quad (2)$$

The ion momentum equation in the radial direction is:

$$\begin{aligned} \frac{\partial}{\partial t} [\rho u_r] + \frac{1}{A_r} \frac{\partial}{\partial r} [A_r (\rho u_r^2 + p_i + p_e)] + \frac{1}{r A_\theta} \frac{\partial}{\partial \theta} [A_\theta \rho u_r u_\theta] \\ = F_r^i + F_r^e + u_r^0 S_c - u_r S_1 + \frac{(p_i + p_e)}{A_r} \frac{\partial A_r}{\partial r} \end{aligned} \quad (3)$$

The ion momentum equation in the angular direction is:

$$\begin{aligned} \frac{\partial}{\partial t} [\rho u_\theta] + \frac{1}{A_r} \frac{\partial}{\partial r} [A_r \rho u_r u_\theta] + \frac{1}{r A_\theta} \frac{\partial}{\partial \theta} [A_\theta (\rho u_\theta^2 + p_i + p_e)] \\ = F_\theta^i + F_\theta^e + u_\theta^0 S_c - u_\theta S_1 + \frac{(p_i + p_e)}{r A_\theta} \frac{\partial A_\theta}{\partial \theta} \end{aligned} \quad (4)$$

Table 1. Ion chemical reaction rates

Reaction	Rate constant ($cm^3 sec^{-1}$)
(R1) $CO_2^+ + O \rightarrow O^+ + CO_2$	1.0×10^{-10}
(R2) $CO_2^+ + O \rightarrow O_2^+ + CO$	1.64×10^{-10}
(R3) $CO_2^+ + e \rightarrow CO + C$	$1.14 \times 10^{-4} T_e$
(R4) $O^+ + CO_2 \rightarrow O_2^+ + CO$	9.4×10^{-10}
(R5) $O^+ + H \rightarrow H^+ + O$	$2.5 \times 10^{-11} T_n^{1/2}$

¹ on leave from Central Research Institute for Physics, Budapest, 1525, Hungary

The ion energy equation is:

$$\begin{aligned} & \frac{\partial}{\partial t} \left[\frac{\rho}{2} (u_r^2 + u_\theta^2) + \frac{p_i}{\gamma_i - 1} \right] + \frac{1}{A_r} \frac{\partial}{\partial r} \left[A_r u_r \left(\frac{\rho}{2} (u_r^2 + u_\theta^2) + \frac{\gamma_i}{\gamma_i - 1} p_i \right) \right] \\ & + \frac{1}{r A_\theta} \frac{\partial}{\partial \theta} \left[A_\theta u_\theta \left(\frac{\rho}{2} (u_r^2 + u_\theta^2) + \frac{\gamma_i}{\gamma_i - 1} p_i \right) \right] + u_r \frac{\partial p_e}{\partial r} + u_\theta \frac{\partial p_e}{r \partial \theta} \\ & = Q_i + u_r (F_r^i + F_r^e) + u_\theta (F_\theta^i + F_\theta^e) + \frac{\partial}{\partial r} \left(K_i \frac{\partial T_i}{\partial r} \right) + \frac{\partial}{r \partial \theta} \left(K_i \frac{\partial T_i}{r \partial \theta} \right) \\ & + \left(\frac{u_r^2}{2} + \frac{u_\theta^2}{2} + \frac{k T_n}{(\gamma_i - 1) m_i} \right) S_c - \left(\frac{u_r^2}{2} + \frac{u_\theta^2}{2} + \frac{p_i}{(\gamma_i - 1) \rho_i} \right) S_i \end{aligned} \quad (5)$$

The electron energy equation is:

$$\begin{aligned} & \frac{\partial}{\partial t} \left[\frac{p_e}{\gamma_e - 1} \right] + \frac{1}{A_r} \frac{\partial}{\partial r} \left[A_r u_r \frac{\gamma_e}{\gamma_e - 1} p_e \right] + \frac{1}{r A_\theta} \frac{\partial}{\partial \theta} \left[A_\theta u_\theta \frac{\gamma_e}{\gamma_e - 1} p_e \right] \\ & - u_r \frac{\partial p_e}{\partial r} - u_\theta \frac{\partial p_e}{r \partial \theta} \\ & = Q_e + \frac{\partial}{\partial r} \left(K_e \frac{\partial T_e}{\partial r} \right) + \frac{\partial}{r \partial \theta} \left(K_e \frac{\partial T_e}{r \partial \theta} \right) + \frac{k T_n}{(\gamma_e - 1) m_e} S_c - \frac{p_e}{(\gamma_e - 1) \rho_e} S_i \end{aligned} \quad (6)$$

where

r	radial component;
θ	angular component;
subscript i	ions;
subscript e	electrons;
subscript n	neutrals;
ρ	mass density ($=\rho_i = \rho_e m_i/m_e$)
A_r, A_θ	area function in radial and angular direction, respectively, ($A_r = r^2$; $A_\theta = \sin \theta$);
S_c, S_i	ion production and loss rate, respectively;
u_r, u_θ	plasma velocity
p	pressure;
γ	specific heat ratio;
F_r^i, F_θ^i	ion force term
F_r^e, F_θ^e	electron force term
k	Boltzmann constant;
m	mass;
T	temperature;
K	thermal conductivity;
Q_i	net ion heating rate,
Q_e	net electron heating rate,
u_r^0, u_θ^0	bulk velocity of the newly created species.

Spherical geometry is used and axial symmetry around the sun-Venus axis is assumed. The use of these "five moment" transport equations clearly limits the accuracy of the results obtained from this model. The use of these equations implies that the temperatures are assumed to be isotropic, the heat flow tensor is replaced by simple thermal conductivities, the flow is inviscid etc; nevertheless this model still gives a good first order description of the major processes controlling the ionospheric dynamics.

Numerical Scheme

The coupled system of equations (2)-(6) are solved numerically for ion densities (ρ), vertical and horizontal velocities (u_r, u_θ), ion temperatures (T_i) and electron temperatures (T_e). The second order accurate Godunov type scheme, which can handle the shock simulation, is used along with a Crank-Nicholson scheme for handling thermal conduction and heat sources in the energy equations and a Runge-Kutta method is employed for handling other source terms. The Crank-Nicholson scheme is second-order accurate and the Runge-Kutta scheme used is third-order accurate, which in effect give us the overall second order accurate solutions. Similar application of the Godunov type scheme was used by Körösmezey and Gombosi [1989] for their two-dimensional cometary atmosphere model.

Boundary and Initial Conditions

The upper boundary is set at 500 km altitude, and the lower boundary is set at 150 km. The two side boundaries are at solar zenith angles (SZA) of 0° and 180° . The vertical and horizontal resolution is 5 km and 5° SZA, respectively. For ion densities (ρ), chemical and diffusive equilibrium conditions are applied at the lower and upper boundaries, respectively. For vertical velocities (u_r), the conditions $u_r=0$ and $\partial u_r/\partial r=0$, are imposed at the upper boundary on the day and nightside respectively, but no flows into the system are allowed. Vertical (u_r) and horizontal velocities (u_θ) are kept equal to zero at the lower boundary. The floating boundary condition, $\partial u_\theta/\partial r=0$ is imposed at the upper boundary for the horizontal velocities (u_θ). For ion and electron temperature (T_i, T_e), the heat fluxes, $\phi = -K \partial T/\partial r$, are set at the upper boundary. T_i and T_e are set equal to the neutral temperatures (T_n) at the lower boundary. The floating boundary conditions ($\partial \rho/r \partial \theta=0$; $\partial u_r/r \partial \theta=0$; $\partial T_i/r \partial \theta=0$; $\partial T_e/r \partial \theta=0$) are set at the side boundaries (SZA = 0° , 180°), except that the horizontal velocities (u_θ) have reflective boundary conditions ($u_\theta, i, n+1 = -u_\theta, i, n$) at SZA = 180° .

In order to establish confidence in our model, a number of different test runs were carried out. In one case we dropped all the source terms and perturbed the density to check if the propagation speed is equal to the sonic speed. A test run with all the source terms included was also carried out for the case of no horizontal variations of the input data (photoionization rates, neutral densities, and photoelectron heating rates) to compare with previous one-dimensional model results. The results of these pseudo one-dimensional calculations are used as the initial conditions for the two-dimensional calculations. A more detailed description of the numerical method can be found in Kim [1991].

Input Parameters

All input parameters for the model are for solar cycle maximum conditions ($F_{10.7} = 200$). The neutral densities are from Hedin et al., [1983] except for the H densities, which were taken from VIRA (Venus International Reference Atmosphere) [Keating et al., 1985] and extrapolated (VIRA only gives densities for $F_{10.7} = 150$ conditions). The presence of hot oxygen is neglected. Photoionization rates and electron heating rates are calculated at every 5° SZA and 5 km altitude grids using the two-stream model of Nagy and Banks [1970]. Ion production rates were arbitrarily decreased from 90° to 100° SZA by a factor of 100 and remained constant after 100° SZA in order to remove the effect of photoionization on the nightside. On the nightside, the electron heating rates are set to the values at the terminator in order to approximate the heating due to the transported photoelectrons and precipitating energetic electrons.

Results and Discussions

The computer intensive nature of this model allowed only a limited number of test cases to be run, therefore the input parameters and boundary conditions could not be "tuned for the best" results, in terms of an overall agreement with observations. However the initial use and purpose of this model is to establish the nature of the transterminator ion flow and related energetics in a quantitative and self consistent manner, rather than fit the observed values exactly. Such studies will be carried out in the future, as further computer resources become available. Also some of the effects neglected in these first calculations (e.g. the presence of hot oxygen atoms) will be included in the work to be presented in a planned, more comprehensive paper. In this short paper we present the results from only one test run, which reproduced the observations in a reasonable but not exact fashion.

A number of studies showed that heating mechanism(s) other than those due to solar EUV radiation must be considered in the study of the energy balance of the Venus and Mars ionospheres [e.g. Chen et al., 1978; Cravens et al., 1980; Kim et al., 1990]. There have also been suggestions that the required heat inflow on the nightside should be smaller than that on the dayside [e.g. Whitten et al., 1986]. For the case presented here constant heat fluxes of 5×10^9 eV $\text{cm}^{-2} \text{s}^{-1}$ for electrons and 2×10^7 eV $\text{cm}^{-2} \text{s}^{-1}$ for ions are imposed at the top boundaries over the dayside and reduced to 30% of these values on the nightside. The model provides O^+ densities, horizontal and vertical velocities and ion and electron temperatures; these are shown in Figure 1(a)-(d).

The calculated ion temperatures are shown in Figure 1(a). At the subsolar point, T_i is about 2000°K , decreases with increasing SZA

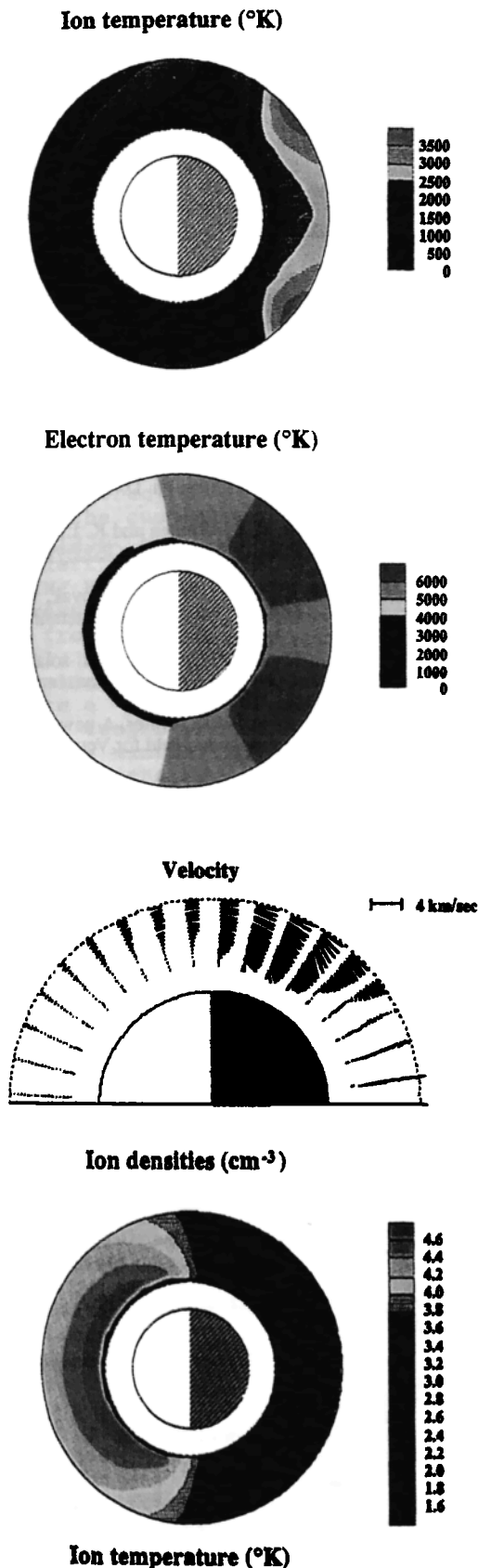


Fig. 1 (a) Color-shaded contour plot of calculated ion temperatures, (b) plot of calculated electron temperatures, (c) vector plot of calculated velocity fields, and (d) plot of logarithm of calculated ion densities.

for $SZA < 100^\circ$ and increases with SZA in the nightside, up to 4000°K partially due to the convergence of the transonic horizontal flows. There is a drop in the calculated ion temperatures in the region between $90\text{-}100^\circ\text{SZA}$ as shown in Figure 1(a) due to the adiabatic expansion of the horizontal flow in the region [Knudsen et al., 1980]. Miller et al.[1980] also found some evidence of a slight cooling in the region immediately antisunward of the terminator. There is also a small drop in the ion temperatures past the shock, which is caused by a small increase in the model neutral densities near the antisolar point and adiabatic cooling resulting from the radially outward flow.

The calculated electron temperatures shown in Figure 1(b) are roughly comparable to the measured values, but are somewhat higher on the nightside because the assumed heat inflows are too large for the low density plasma on the nightside. The variation of the electron temperatures are within about 3000°K across all SZA range. The median of the observed T_e show little variation over all SZAs [Miller et al., 1980]. In the dayside Venus ionosphere, the two heat sources considered are the topside heat flow and the photoelectron heating. The latter decreases as SZA increases on the dayside and drops sharply after the terminator, unless the effect of energetic electron precipitation is included. Thus the T_e would decrease monotonically from the subsolar to antisolar point without an assumed topside heat flow.

The calculated velocity fields shown in Figure 1(c) reach supersonic values up to 3.5 km sec^{-1} , which are in reasonably good agreement with the measurements [Knudsen et al., 1982]. The horizontal velocities at 397.5 km are shown in Figure 2 together with the observed values at 400 km taken from Whitten et al., [1984]. The flow has to be slowed down before it reaches the antisolar region. A shock wave is formed at around 135° SZA , which can be seen in the vector plot shown in Figure 1(c). Beyond the shock wave, the ion density builds up only slightly [see Figure 1(d)] because horizontally transported ions are lost via recombination. There are strong downward motions on the nightside, with a maximum downward speed of about 600 m sec^{-1} .

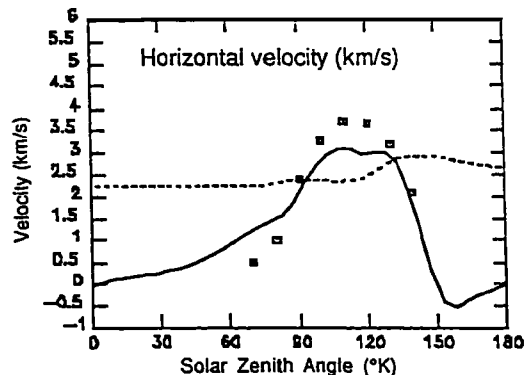


Fig. 2 Calculated horizontal velocities (solid) with sonic speed (dotted) at the altitude of 397.5 km . Squares are the observed horizontal velocities at 400 km taken from Whitten et al. [1984].

The flow at the top boundaries on the nightside was not prescribed, but was free to float, while the radial flow on the dayside was kept at zero. This top boundary condition for the radial flow, together with the decreasing ion-neutral friction with SZA and mass sink, accelerate the already expanding flow further. Downward motions are dominant in the region between 90° and 150° SZA , which can be explained with the stronger O^+ loss at lower altitudes compared to at higher altitudes on nightside. The shock wave front is tilted because the flow stops at lower altitudes earlier than at higher altitudes due to the friction provided by the denser neutral atmosphere at lower altitudes, especially the hydrogen which has a nightside bulge. In a test run without the hydrogen component, the shock wave front was not tilted and was located further away at around 160° SZA . Beyond the shock wave, there are relatively weaker ($\sim 200\text{ m sec}^{-1}$) upward motion at all altitudes, allowing the plasma to escape into the tail.

The calculated ion densities shown in Figure 1(d) decrease with increasing SZA up to about 150° SZA and increase slightly with respect to SZA beyond about 150° SZA. The calculated ion densities above 200 km drop by about a factor of 600 from 0° to 150° SZA. Both the peak O⁺ density and the altitudes of the peak ion density tend to decrease with increasing SZA due to the increasing downward motion from the day to nightside. The photoionization rates of O⁺ and CO₂⁺ remain almost constant on dayside and start to drop sharply after 80° SZA. The ion production rate on the nightside is practically zero. Thus in this model calculation, transport from dayside across the terminator maintains the nightside ionosphere shown in Figure 1(d). Our model includes the loss O⁺ by charge exchange to H, but not the reverse source reaction. A test run which eliminated this loss term, resulted in a fourfold increase in the nightside ion densities. Furthermore we use an upper boundary of 500 km; earlier calculations [e.g. Cravens et al., 1983] showed that increasing the effective ionopause altitude leads to higher transterminator fluxes and nighttime densities. Finally it was shown by McCormick et al., [1987] that the nightside densities are very sensitive to the neutral density model used; they could not reproduce the observed densities with the Hedin et al. [1983] model, which was used in this work.

The total height integrated plasma flux across the terminator was evaluated and found to be about 1×10^{26} particles sec⁻¹. This value is very nearly equal to the total loss rate integrated over the night side, because the integrated escape flux (which occurs between about 150° and 180° SZA) is only about 1×10^{24} particles sec⁻¹.

Conclusions

The first full-scale, self-consistent two-dimensional calculations capable of handling shock waves were carried out for the Venus ionosphere, corresponding to solar cycle maximum conditions. This model successfully simulates the plasma flow over the 0-180° SZA range, where traditional numerical scheme could not properly handle the region beyond 150° SZA.

It was again demonstrated that the introduction of topside heat inflows leads to calculated dayside electron and ion temperatures, which are consistent with the measured values. In order to reproduce the measured electron temperatures, which is roughly constant over all SZA's, the heat inflows had to be reduced significantly over the nightside compared to the dayside values.

The model predicts lower ion densities on the nightside than the measured ones; this is believed to be due to 1) the inclusion of the charge exchange loss but not the source reaction, 2) the use of an effective ionopause which is too low and 3) the choice of the neutral atmosphere model. These issues will be addressed in the planned future work, mentioned earlier.

The calculated transterminator ion flows are supersonic and relatively close to the observed average values. The model predicts a deceleration shock at a SZA of about 135°, consistent with the ion temperature and velocity observations.

Acknowledgements

The work presented in this paper was supported by NASA Grants NAG2-491 and NAGW-1619. Acknowledgement is made to the National Center for Atmospheric Research, which is sponsored by the National Science Foundation, and the San Diego Supercomputer Center for computation resources.

References

- Chen, R.H., Cravens, T.E., and Nagy, A.F., The Martian ionosphere in light of the Viking observations, *J. Geophys. Res.*, **83**, 3871, 1978.
- Colin, L., The Pioneer Venus program, *J. Geophys. Res.*, **85**, 7575, 1980.
- Cravens, T.E., Gombosi, T.I., Kozyra, J.U., and Nagy, A.F., Model calculations of the dayside ionosphere of Venus: Energetics, *J. Geophys. Res.*, **85**, 7778, 1980.
- Cravens, T. E. S. L. Crawford, A. F. Nagy and T. I. Gombosi, A two-dimensional model of the ionosphere of Venus, *J. Geophys. Res.*, **88**, 5595, 1983.
- Gombosi, T.I., Cravens, T.E., and Nagy, A.F., A time-dependent theoretical model of the polar wind: Preliminary results, *Geophys. Res. Lett.*, **12**, 167, 1985.
- Hedin, A.E., Niemann, H.B., Kasprzak, W.T., and Seiff, A., Global empirical model of the Venus thermosphere, *J. Geophys. Res.*, **88**, 73, 1983.
- Keating, G.M., Bertaux, J.L., Bougher, S.W., Cravens, T.E., Dickinson, R.E., Hedin, A.E., Krasnapolsky, V.A., Nagy, A.F., Nicholson, J.Y., Paxton, L.J., and Zahn, U.v., Models of Venus neutral upper atmosphere: Structure and composition, *Adv. Space Res.*, **5**, 117, 1985.
- Kim, J., A. F. Nagy, T. E. Cravens and H. Shinagawa, Temperature of individual ion species and heating due to charge exchange in the ionosphere of Venus, *J. Geophys. Res.*, **95**, 6569, 1990.
- Kim, J., Model studies of the ionosphere of Venus: Ion composition, energetics and dynamics, Ph. D. Thesis, U. of Michigan, 1991.
- Knudsen, W. C., K. Spenner, R. C. Whitten and K. L. Miller, Ion energetics in the Venus nightside ionosphere, *Geophys. Res. Lett.*, **7**, 1045, 1980.
- Knudsen, W.C., Spenner, K., Miller, K.L., and Novak, V., Transport of ionospheric O⁺ ions across the Venus terminator and implications., *J. Geophys. Res.*, **85**, 7803, 1980.
- Knudsen, W.C., Spenner, K., and Miller, K.L., Anti-solar acceleration of ionospheric plasma across the Venus terminator, *Geophys. Res. Lett.*, **8**, 241, 1981.
- Knudsen, W. C., P. M. Banks and K. L. Miller, A new concept of plasma motion and planetary magnetic field for Venus, *Geophys. Res. Lett.*, **2**, 765, 1982.
- Körösmezey, A., and Gombosi, T.I., A time dependent dusty-gas dynamic model of axisymmetric cometary jets, *Icarus*, **84**, 118, 1989.
- McCormick, P. T., R. C. Whitten and W. C. Knudsen, Dynamics of the Venus ionosphere revisited, *Icarus*, **70**, 469, 1987.
- Miller, K.L., Knudsen, W.C., Spenner, K., Whitten, R.C., and Novak, V., Solar zenith angle dependence of ionospheric ion and electron temperatures and density on Venus, *J. Geophys. Res.*, **85**, 7759, 1980.
- Nagy, A.F., and Banks, P.M., Photoelectron fluxes in the ionosphere, *J. Geophys. Res.*, **75**, 6260, 1970.
- Whitten, R.C., McCormick, P.T., Merritt, D., Thompson, K.W., Brynsvold, R.R., Eich, C.J., Knudsen, W.C., and Miller, K.L., Dynamics of the Venus ionosphere: A two-dimensional model study, *Icarus*, **60**, 317, 1984.
- Whitten, R.C., Singhal, R.P., and Knudsen, W.C., Thermal structure of the Venus ionosphere: A two dimensional model study, *Geophys. Res. Lett.*, **13**, 10, 1986.
- A. F. Nagy, J. Kim, T. I. Gombosi, Space Physics Research Laboratory, Department of Atmospheric, Oceanic and Space Sciences, The University of Michigan, Ann Arbor, MI 48109-2143.
- A. Körösmezey, Central Research Institute for Physics, Budapest, 1525, Hungary.

(Received December 28, 1990;
accepted January 24, 1991.)